Published in Journal of Computational Neuroscience, 24 (2), 222-234, 2008.

The role of synaptic facilitation in spike coincidence detection

Jorge F. Mejías and Joaquín J. Torres
Department of Electromagnetism and Physics of the Matter and
Institute "Carlos I" for Theoretical and Computational Physics,
University of Granada, E-18071 Granada Spain.

September 5, 2008

Abstract

Using a realistic model of activity dependent dynamical synapse, which includes both depressing and facilitating mechanisms, we study the conditions in which a postsynaptic neuron efficiently detects temporal coincidences of spikes which arrive from N different presynaptic neurons at certain frequency f. A numerical and analytical treatment of that system show that: i) facilitation enhances the detection of correlated signals arriving from a subset of presynaptic excitatory neurons, and ii) the presence of facilitation yields to a better detection of firing rate changes in the presynaptic activity. We also observed that facilitation determines the existence of an optimal input frequency which allows the best performance for a wide (maximum) range of the neuron firing threshold. This optimal frequency can be controlled by means of facilitation parameters. Finally, we show that these results are robust even for very noisy signals and in the presence of synaptic fluctuations produced by the stochastic release of neurotransmitters.

1 Introduction

Recently it has been reported that postsynaptic potentials recorded in cortical neurons present dynamical properties depending on the presynaptic activity (Tsodyks and Markram, 1997; Abbott et al., 1997). This behaviour can be understood by means of the action of different mechanisms which take place at the level of the synapses, as for instance, short-term depression and/or facilitation. The first mechanism considers that the amount of available neurotransmitters in the synaptic buttons is limited and, therefore, the neuron needs some time to recover these synaptic resources in order to transmit the next incoming spike. As a consequence, the dynamics of the synapse is affected by an activity-dependent mechanism which produces non-linear effects in the postsynaptic response. This picture differs from the classical synaptic description which considers the synaptic strengths as static identities, with the only possible time modification due to a slow learning process (Hopfield, 1982). Moreover,

it is well known that short-term depression plays an important role in several emerging phenomena in the brain, such as selective attention (Buia and Tiesinga, 2005; McAdams and Maunsell, 1999) and cortical gain control (Abbott et al., 1997), and it is responsible for the complex switching behaviour between activity patterns observed in neural network models with depressing synapses (Pantic et al., 2002; Cortes et al., 2006). However, a complete theoretical study of other synaptic mechanisms, as synaptic facilitation –which compete with depression during synaptic transmission in networks of pyramidal neurons– is still lacking. Synaptic facilitation is produced by the influx of calcium ions into the cell through voltage-sensitive channels which favours the neurotransmitter vesicle depletion. This has been reported to be relevant for synchrony and selective attention (Buia and Tiesinga, 2005), and in the detection of bursts of action potentials (AP) (Matveev and Wang, 2000; Destexhe and Marder, 2004). One would expect, therefore, that synaptic facilitation had a positive effect, for instance, in the efficient transmission of temporal correlations between spike trains arriving from different synapses. This feature, known as synaptic coincidence detection (CD), has been measured *in vivo* in cortical neurons and related with some dynamical processes which affect to neuron firing thresholds (Azouz and Gray, 2000), so that it seems to be an important mechanism for efficient transmission of information in actual neural media.

In this work, we used the phenomenological model of dynamic synapses introduced in (Tsodyks et al., 1998), which includes depressing and facilitating mechanisms, to explore the consequences of the cooperative effect of both in spike CD tasks. That is, we computed the regions, in the space of the relevant parameters, in which a postsynaptic neuron can efficiently detect temporal coincidences of spikes arriving from N different afferents. The aim is to determine the range of the parameters which defines the dynamic of the synapses and the neuron for which the performance of the neural system in such experiments is improved. Our study shows that facilitation enhances the detection of correlated spikes and firing rate changes in situations for which the mechanism of depression alone does not perform well. These main results are robust and persist even when one decreases the degree of correlation between the afferents or consider more realistic situations, as for instance, stochastic individual synapses (Dobrunz and Stevens, 1997; de la Rocha and Parga, 2005). Synaptic facilitation also determines the existence of an optimal frequency which allows the best performance for a wide range of values of the neuron firing threshold. The location of this optimal frequency can also be controlled by means of facilitation control parameters. This property could be important for actual neural media, constituted by neurons which presents heterogeneity in their firing thresholds (Azouz and Gray, 2000), to efficiently process information codified, for instance, at this frequency.

2 The model

We consider a postsynaptic neuron which receives signals from N presynaptic neurons through excitatory synapses. As a first approximation to model experimental data, we assume that the stimulus received by a particular neuron, as a consequence of the overall neural activity, is modeled by a spike train following a Poisson distribution with mean frequency f (Tsodyks et al., 1998). According

to the phenomenological model presented in (Tsodyks and Markram, 1997), we consider that the state of the synapse i is governed by the system of equations

$$\begin{aligned} \frac{dx_i}{dt} &= \frac{z_i}{\tau_{rec}} - U_i(t)x_i\delta(t-t_{sp}) \\ \frac{dy_i}{dt} &= -\frac{y_i}{\tau_{in}} + U_i(t)x_i\delta(t-t_{sp}) \\ \frac{dz_i}{dt} &= \frac{y_i}{\tau_{in}} - \frac{z_i}{\tau_{rec}}, \end{aligned} \tag{1}$$

where x_i,y_i,z_i are the fraction of neurotransmitters in a recovered, active and inactive state, respectively. Here, τ_{in} and τ_{rec} are the inactivation and recovery time constants, respectively. Depressing synapses are obtained for $U_i(t) = U_{SE}$ constant, which represents the maximum amount of neurotransmitters which can be released (activated) after the arrival of each presynaptic spike. The delta functions appearing in (1) consider that an AP arrives at the synapse in a fixed time $t = t_{sp}$. Typical values of these parameters in cortical depressing synapses are $\tau_{in} = 3\ ms$, $\tau_{rec} = 800\ ms$, and $U_{SE} = 0.5$ (Tsodyks and Markram, 1997).

The synaptic facilitation mechanism can be introduced assuming that $U_i(t)$ has its own dynamics related with the release of calcium from intracellular stores and the influx of calcium from the extracellular medium each time an AP arrives. Here, we consider the dynamics proposed in (Tsodyks and Markram, 1997), that is,

$$U_i(t) \equiv u_i(t)(1 - U_{SE}) + U_{SE} \tag{2}$$

with

$$\frac{du_i(t)}{dt} = -\frac{u_i(t)}{\tau_{fac}} + U_{SE}[1 - u_i(t)]\delta(t - t_{sp}). \tag{3}$$

Here, $u_i(t)$ is a dynamical variable which takes into account the influx of calcium ions into the presynaptic neuron near the synapse through voltage-sensitive ion channels (Bertram et al., 1996). These ions can usually bind to some acceptor which gates and facilitates the release of neurotransmitters. A typical value for the facilitation time constant is $\tau_{fac} = 530\ ms$ (Markram et al., 1998). The variable $U_i(t)$ in (2) represents then the maximum fraction of neurotransmitters that can be activated, either by the arriving of a presynaptic spike (U_{SE}) and by means of facilitating mechanisms (i.e., $u_i(t)(1 - U_{SE})$).

One can think that the postsynaptic current generated in a particular synapse is proportional to the fraction of neurotransmitters which are in the active state, that is, $I_i = A_{SE} \cdot y_i$, where A_{SE} is the maximum postsynaptic current that can be generated [1]. Hereafter, we will choose $A_{SE} \approx 42.5\,pA$ which is within the physiological range and gives an optimal system performance for $V_{th} = 13mV$. In fact, we used this value because is very near to the mean value threshold measured in some cortical areas (Azouz and Gray, 2000). The total postsynaptic current, generated by signals arriving from the N excitatory synapses, can be written, therefore, as $I_{total} = \sum_{i=1}^{N} I_i$. This current generates a postsynaptic

[1] Note that it is the synaptic conductance, rather than the synaptic current, which depends on $A_{SE} \cdot y(t)$. Our assumption for the current, however, is a good approximation when the membrane potential $V(t)$ is below the firing threshold V_{th} and $\tau_m \gg \tau_{in}$, so that $V(t)$ remains constant during the temporal variation of the synaptic conductance.

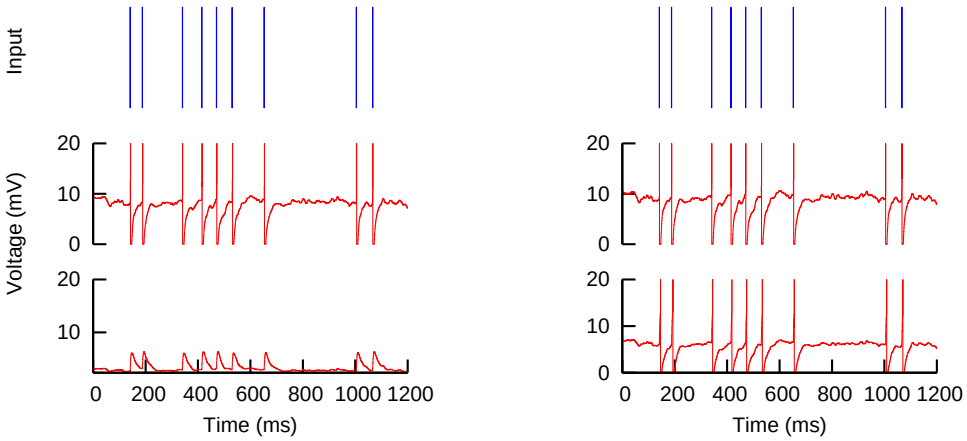

Figure 1: Response of a postsynaptic neuron receiving Poisson spike train (Top panel) at frequency of 10 Hz from $N = 1000$ presynaptic neurons through dynamic synapses. Left and right panels correspond, respectively, to the case of depressing and facilitating synapses. In the simulations, U_{SE} takes the values 0.5 (middle panel)and 0.01 (bottom panel), respectively, and the threshold is fixed to $13\,mV$. The figure shows that facilitation enhances CD tasks for relatively low values of U_{SE}.

membrane potential which we modeled using an integration-and-fire (IF) neuron model, i.e.,

$$\tau_m \frac{dV}{dt} = -V + R_{in} I_{total}, \tag{4}$$

where $R_{in} = 0.1\,G\Omega$ and $\tau_m = 15\ ms$ are, respectively, the input resistance and the membrane time constant. These typical values have been taken also from pyramidal cells (Tsodyks and Markram, 1997). The IF neuron model assumes that, once the membrane potential reaches a certain threshold V_{th}, above the resting potential $V_{rest} = 0$, an AP is generated and $V(t)$ is reset to zero. We assume, in addition, the existence of a refractory period of $\tau_{ref} = 5\ ms$ during which $V(t)$ remains in zero after the generation of each postsynaptic AP.

3 Detection of strongly correlated signals

We have studied first the postsynaptic response of a neuron receiving input signals from $N = 1000$ excitatory synapses, with a subset of $M = 200$ synapses stimulated by identical spike trains with mean frequency f. These strongly correlated afferents fire spikes which are synchronized in time and we consider them as a *signal* term. The remaining $N-M$ synapses receive uncorrelated spike trains (also with mean frequency f) which constitute, therefore, a *noisy* background of activity which is added to the signal. We have investigated, both analytically and numerically, spike coincidence detection (CD) experiments. Our interest is to determine the values of the synapse and neuron parameters for which the postsynaptic neuron can detect the embedded signal, i.e., its response is strongly correlated with the input signal.

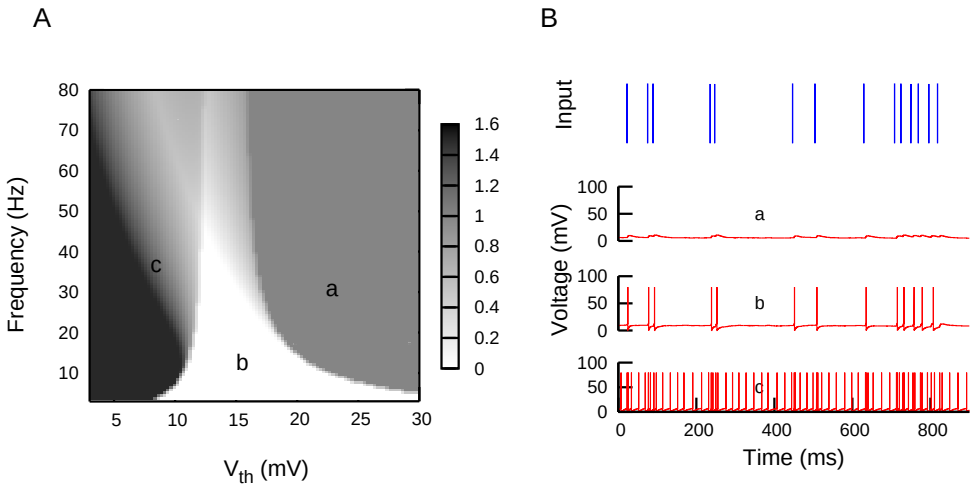

Figure 2: Panel A shows a typical coincence detection map, as defined in the text, with depressing synapses ($U_{SE} = 0.5$, $\tau_{rec} = 800$ and $\tau_{fac} = 0$). Panel B depicts the corresponding temporal behaviour of the postsynaptic membrane potential for several situations marked in the map with labels. It shows examples of failures in the detection (a), successful detections or hits (b) and false spikes (c). Situations (a) and (c) correspond in the map to high error zones.

A typical CD experiment is illustrated in Fig. 1. This shows the effect of including facilitation compared with the situation in which only depression is considered. For relatively high values of the parameter U_{SE}, the system presents good performance in the CD of the incoming signals for both cases, and the simulations do not show any remarkable differences when one includes facilitation. The reason is that the facilitation term becomes irrelevant in Eq. 2 for high values of U_{SE}, and depression is the only mechanism contributing to the dynamics. For small U_{SE}, however, the detection of the signal is improved in the presence of the facilitating mechanism. In fact, when U_{SE} takes low values, the contribution of depression to $U_i(t)$ –which gives the strength of the synapse– becomes irrelevant. In this situation, facilitation still contributes to maintain $U_i(t)$ highly enough to allow a good performance on the CD task.

For a more general evaluation and quantification of the role of the facilitating mechanism, we computed the fraction of errors that occur in the detection of the presynaptic signal by the postsynaptic neuron as a function of the incoming frequency f and the neuron threshold V_{th}. These 2-dimensional CD error *maps* give a better perspective of the regions, in the space of the relevant parameters, where the system has good performance. Thus, for each pair (f, V_{th}), we computed, in the stationary regime and during a large temporal interval T, 1) the number of coincidence-input-events produced by strongly correlated signals through M presynaptic neurons, namely $N_{inputs} \equiv f \cdot T$, 2) the number of output spikes in the postsynaptic neuron which occur immediately within a time-window of $\Delta = 5\ ms$ after each coincidence-input-event, that is N_{hits},[2]

[2]The specific value of Δ is not too critical for the results found if moderated values are used. In particular, it is convenient to have $\Delta \sim \tau_{ref}$ since this is a natural window for spike

3) the number of output spikes which are not hits, N_{falses}, and finally 4) the number of coincidence-input-events which did not result in output spikes within the time window Δ, namely $N_{failures}$ (Pantic et al., 2003). The fraction of errors is then defined as

$$E(f, V_{th}) \equiv \frac{N_{failures} + N_{falses}}{N_{inputs}}. \tag{5}$$

Analytical expressions for the quantities appearing in (5) have been obtained by integration of the model equations (1-4) and their derivation is explained in the appendix.

We have computed both theoretical and numerical CD maps using the error function (5) for different values of the neuron and synapse relevant parameters. An illustrative example of these maps is shown in Fig. 2A. The light area corresponds to regions where the postsynaptic neuron is able to efficiently detect the coincidence-input-events, and to generate a postsynaptic response strongly correlated with the embedded signal (see time series "b" on Fig. 2B). Simulations show that this mainly occurs for $E \lesssim 0.6$. Dark areas, however, are regions with a high percentage of errors ($E \geqslant 1$). These errors can be produced, for instance, when $N_{failures}$ is large (see time series "a" on Fig. 2B), which occurs for V_{th} very large (grey areas), or when N_{falses} increases (see time series "c" on Fig. 2B), normally for small V_{th}, such that any current can produce a false event (black areas). Figure 3 depicts the role of the inclusion of synaptic facilitation on signal detection compared with the situation of only depressing synapses. For a fixed value of the facilitation time constant τ_{fac}, there is a clear dependence on U_{SE} in the signal detection properties of the system. When its value increases (from top to bottom) the width of the light area enlarges and spreads to the right, allowing a better CD for regions with high thresholds. The left panels correspond to numerical simulations whereas the central panels are the same error function evaluated using the analytical formulas derived in the appendix. The figure also shows the good agreement between theory and simulations. In the right panels, we computed the same CD maps but considering only the mechanism of synaptic depression. One observes that for only depression and a limited amount of neurotransmitters ($U_{SE} < 0.5$), the low-error region is narrower, and one has a large region of good detection only for U_{SE} near to one. Similar results are found when one fixes U_{SE} and varies τ_{fac}.

A better quantification of the role of synaptic facilitation can be visualized by computing the area of the light zones in the CD maps (low error zones, that is, $E(f, V_{th}) < E_0 = 0.5$), and study the influence of τ_{fac} and U_{SE} on the size of this area. Large light areas will indicate good performance of the system for a large variety of working frequencies and neuron firing thresholds. For this purpose we defined the quantity

$$F = 1 - \frac{1}{A} \int_{V_{th}} \int_{f} \frac{1}{2} \left\{1 + \theta[E(f, V_{th}) - E_0]\right\} dV_{th} df, \tag{6}$$

which gives the fraction of area with small errors over the whole map. Here, $A = \int_{V_{th}} \int_{f} dV_{th} df$ is the total area of the map and $\theta(x)$ is the step function. Figure 4 shows the dependence of F with τ_{fac} (left panel) and U_{SE} (right

detection.

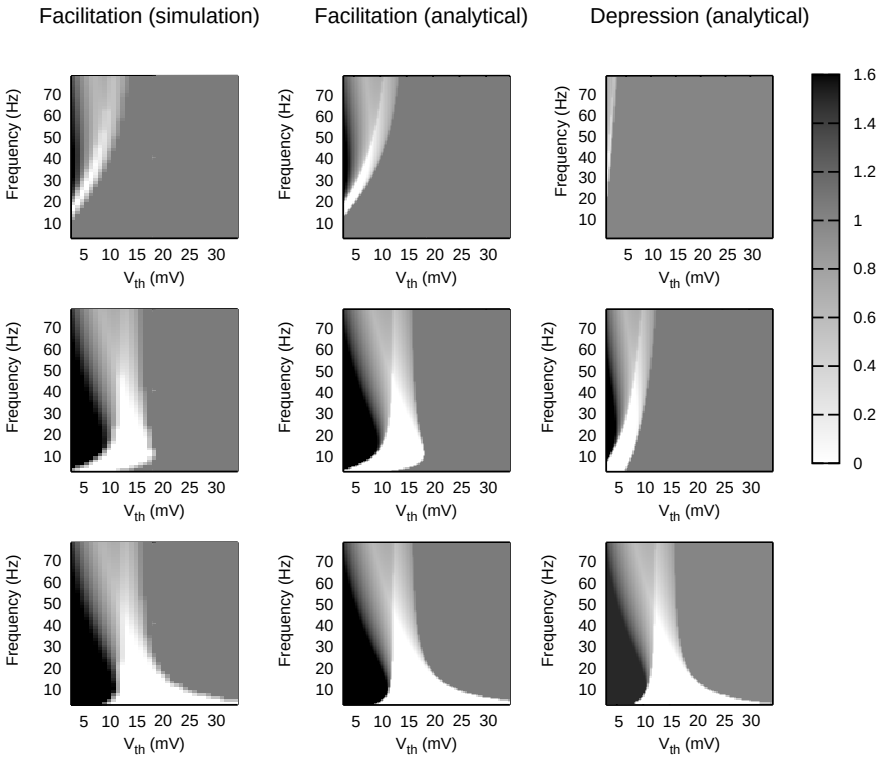

Figure 3: Coincidence detection maps for a system with facilitating synapses with $\tau_{fac} = 530\,ms$ (left and center panels). The values of U_{SE} were, from top to bottom, 0.002, 0.05 and 0.5, respectively. The effect of increasing U_{SE} was the spreading of the region of good CD (light zone) to the right. Simulations (left) confirm the analytical results (center). In the right panels are presented the same CD maps for $\tau_{fac} = 0$, that is, the case of only depressing synapses.

panel). Since F is an increasing function of τ_{fac} (left panel) and the only-depression case corresponds to $\tau_{fac} = 0$, one conclude that the inclusion of facilitation leads to a higher area of good CD in the maps, for different values of U_{SE}. Similar results are found when one study F as a function of U_{SE} (right panel). In this graph, the lowest curve corresponds to the case of only depressing synapses ($\tau_{fac} = 0$), and one observes that the addition of facilitation always leads to a higher F for any value of U_{SE}. These results are also robust for different values of E_0 and different sizes of the (f, V_{th})-window which we use to calculate the total area. All these results show that for the same value of the amount of activated neurotransmitters the overall performance of the system is better with facilitation than if one only consider depressing mechanisms. This conclusion can be also observed when one fixes U_{SE} and varies the facilitation time constant τ_{fac}. A large value for τ_{fac} means an increase in the duration of the facilitating effect. As a consequence, the region for good detection enlarges

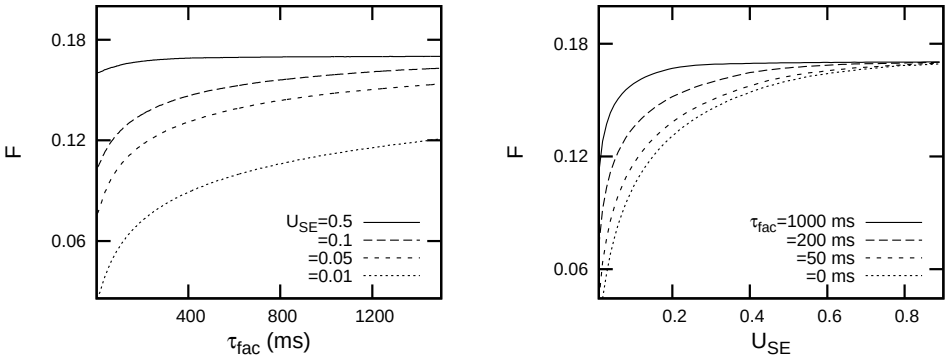

Figure 4: Fraction of area for good signal detection (that is, the region in which the error is below a certain value E_0) as a function of τ_{fac} (left plot) or U_{SE} (right plot), with $E_0 = 0.5$. Both maps show quantitatively that the inclusion of facilitation enlarges the area in which the signal is efficiently transmitted (note that the case of only depressing synapses corresponds to $\tau_{fac} = 0$). The window considered to calculate the area was $f\epsilon[1, 80]$, $V_{th}\epsilon[1, 35]$.

compared with the situation of only depression, in special when the fraction of available resources is not too high.

A detailed observation of Fig. 3 also reveals the existence of a certain frequency, namely f_{opt} which allows a good performance for a wide (maximum) range of values of V_{th}. The center map in Fig. 3, for instance, shows a good performance in detecting signal frequencies around 7 Hz for a threshold ranging from 8 to 18 mV. The existence of this *optimal* frequency can be seen more clearly if we take several sections of the CD maps, with V_{th} fixed at certain value, as it is shown in Fig. 5. For depressing-facilitating synapses (left panel in the figure) there is a certain frequency value (~ 7 Hz) for which the error is zero for very different voltage threshold values within the range $(10 - 17\ mV)$. This feature is not found in the case of only depressing synapses (right panel in the figure). Theoretically, f_{opt} can be computed from the analytical expression for V_{signal} and V_{noise} (see appendix) taking into account that, in general, it appears at relatively low frequencies. At these frequencies, the low error zone is obtained for $V_{th} \in [V_{noise}, V_{noise} + V_{signal}]$. Maximizing this range gives f_{opt}, as the solution of the equation

$$\left| \frac{\partial V_{signal}(f)}{\partial f} \right|_{f=f_{opt}} = 0. \tag{7}$$

A more detailed study using (7) reveals that f_{opt} decreases for increasing values of U_{SE}, or τ_{fac}, as it is shown in Fig. 6 (Left panel). One also observes that the range of thresholds which allow for a good CD at f_{opt}, namely $\Delta V_{th} \approx V_{signal}(f_{opt})$, increases with U_{SE}, or τ_{fac} (cf. Fig. 6 right panel). In the limit $\tau_{fac} \gg 1$, one expects, therefore, the larger ΔV_{th} at f_{opt} near zero. For low

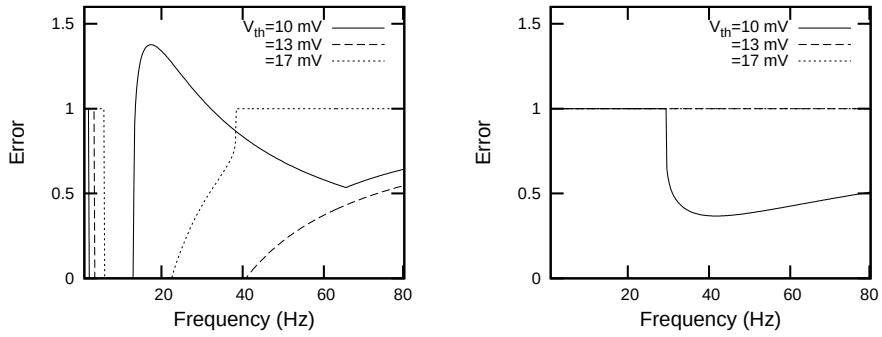

Figure 5: Behaviour of the error function $E(f, V_{th})$ for $U_{SE} = 0.05$ and three values of V_{th}, namely, 10 mV (solid line), 13 mV (dashed line) and 17 mV (dotted line). Left(Right) panel corresponds to depression-facilitation (only depression) case. Considering only these threshold values, one already obtains a small region of frequencies that allow to have zero error for the three threshold values. Indeed, there is a maximum interval of threshold values from 9 to 18 mV such that, this small region of frequencies tends to a single "optimal" frequency around 7 Hz.

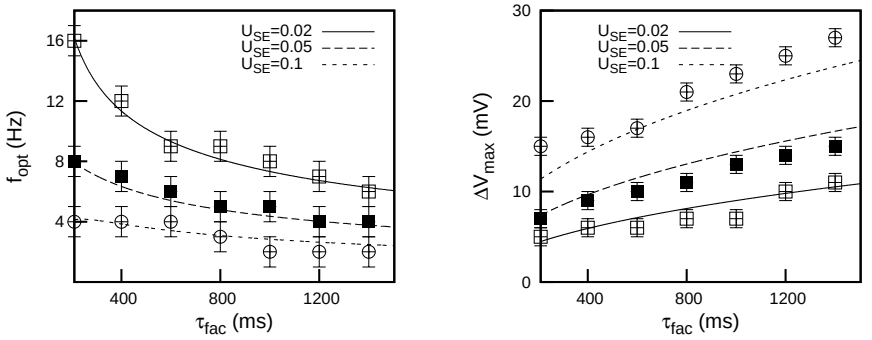

Figure 6: Dependence of f_{opt} and the corresponding threshold-window of good CD, ΔV_{th}, with the facilitation parameters τ_{fac} and U_{SE}. The graph show that f_{opt} can be tuned by means of the facilitation parameters. The figure also shows the agreement between theory (lines) and simulations (symbols).

levels of facilitation, however, there is a critical value of τ_{fac}, such that ΔV_{th} at f_{opt} starts to become lower than ΔV_{th} at zero frequency, and we have, then, $f_{opt} = 0$ (data not shown). For only depressing synapses, i.e., $\tau_{fac} = 0$, one has always $f_{opt} = 0$. The conclusion is that a moderate level of facilitation is needed in order to have a non-zero f_{opt}. The possibility to tune this optimal frequency

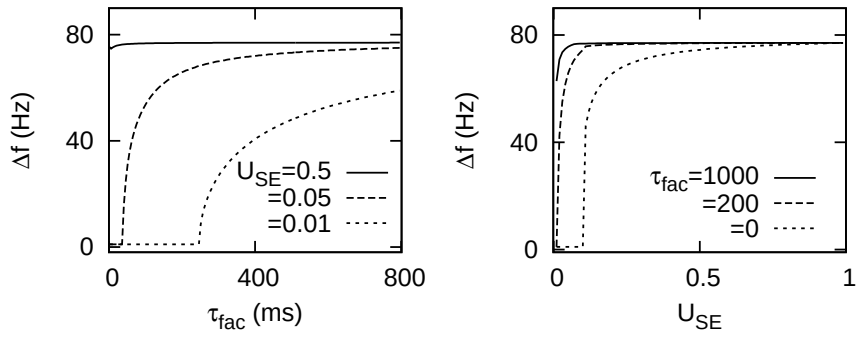

Figure 7: Variation of Δf, as defined in the text, for different values of U_{SE} and τ_{fac}. Left: Δf as a function of τ_{fac} for three fixed values of U_{SE}. Right: Δf as a function of U_{SE} for three fixed values of τ_{fac}. In all cases V_{th} was set to $13\,mV$. In both panels the only-depression case corresponds to $\tau_{fac} = 0$.

by means of the facilitation parameters could be important, for instance, to understand how actual neural systems –where different types of neurons may have non-identical firing thresholds– can self-organize to efficiently detect and process correlated signals at this optimal frequency.

By direct observation of the CD maps, one also observes that, at certain threshold, there is a range of working frequencies, namely Δf, within which the neuron is able to efficiently detect and process incoming signals (with errors, for instance, less than 0.5). The study of the variation of Δf in the presence of facilitation and/or depression tell us, for instance, the ability of the neuron to detect or not complex signals that include many frequencies. In Fig. 7 we have performed this analysis for a fixed threshold around $V_{th} = 13\,mV$ –which is within the physiological range in cortical neurons– and study the system behaviour for fixed U_{SE} and varying τ_{fac} and vice versa. The figure shows (left panel) that Δf decreases with U_{SE} for the case of only depressing synapses, and even vanishes for $U_{SE} < 0.05$. However, if the facilitating mechanism is also present the system is able to recover the good performance by increasing the facilitation time constant. The figure also reveals (right panel) that facilitation always enlarges the maximum range of frequencies for any fixed value of U_{SE}. We conclude that for any values of the synapse parameters the inclusion of facilitation improves the detection towards wider ranges of frequencies. Note that there is an abrupt change, from zero to nonzero values of Δf, in both panels of the Fig (7) when one varies the synapse parameters U_{SE} or τ_{fac}. The reason is that the analysis has been performed for V_{th} fixed around $V^* = 13\,mV$. Then, one has $\Delta f = 0$ for values of U_{SE} and τ_{fac} such that the region of good detection occurs at thresholds smaller than V^* and, therefore, none frequency range is detected at V^*. Otherwise, non-zero Δf start to appear when, by increasing U_{SE} or τ_{fac}, the light area of the map spreads to higher threshold values and reaches V^*.

4 The effect of jitter and synaptic fluctuations

Detection of coincident signals which arrive from different presynaptic neurons have been treated in the previous section in an approximate way, i.e., the embedding signal was constituted by fully correlated temporal events that produce synchronized responses. In real situations, however, the incoming signals from different synapses do not produce strong correlated postsynaptic responses, mainly due to stochasticity during transmission through individual synapses (Dobrunz and Stevens, 1997). The model we used for synaptic transmission does not allow to consider these fluctuations because is deterministic. In this section, however, we explored how the main conclusions reported before are not affected by the inclusion of some desynchronization (jitter) in the signal term which induces fluctuations in the postsynaptic response. We also studied in detail CD tasks with a more realistic stochastic synapse model which naturally induces such fluctuations.

A first step to artificially introduce synaptic fluctuations, or other sources of noise in our system, is to assume a signal term, in the synaptic current, constituted by the effect of M presynaptic events that arrive at random times t_i, distributed around certain time t_0. We used here, for instance, a Gaussian distribution $p(t_i)$ with a certain standard deviation or *jitter* σ. In the following, we consider the implications of this assumption to test the validity of the results previously obtained, and to investigate the effect of the jitter in the detection of signals that are not fully correlated.

We start by computing the excitatory postsynaptic current generated in a synapse i due to a single presynaptic AP occurring at time t_i, i.e.,

$$I_i(t) = I_{peak} \exp[-(t-t_i)/\tau_{in}] \quad t > t_i, \tag{8}$$

where I_{peak} is the steady-state maximum current through a synapse obtained after stimulation with a periodic spike train (see the appendix for details). Since t_i is a Gaussian distributed stochastic variable with $\langle t_i \rangle = t_0$ and standard deviation σ, $q_i(t) \equiv \exp[-(t-t_i)/\tau_{in}]$ (with t fixed) is also a random variable with range $[0,1]$ and probability distribution given by

$$\mathcal{P}[q_i(t)] = \frac{2\tau_{in}}{q_i(t)\ \mathrm{erfc}\left(-\frac{t-t_0}{\sqrt{2}\sigma}\right)} \frac{1}{\sqrt{2\pi}\sigma} \exp\left[-\frac{(t-t_0+\tau_{in}\ln[q_i(t)])^2}{2\sigma^2}\right], \tag{9}$$

where $\mathrm{erfc}(x) = 1 - \mathrm{erf}(x)$ and $\mathrm{erf}(x)$ is the error function. One can easily compute the two first moments for $\mathcal{P}[q_i(t)]$, i.e.:

$$\langle q_i(t) \rangle_q = \exp\left[\frac{1}{2}(\sigma/\tau_{in})^2 - (t-t_0)/\tau_{in}\right] \frac{\mathrm{erfc}\left[\frac{\sigma^2-(t-t_0)\tau_{in}}{\sqrt{2}\sigma\tau_{in}}\right]}{\mathrm{erfc}\left[-\frac{t-t_0}{\sqrt{2}\sigma}\right]}, \tag{10}$$

$$\left\langle [q_i(t)]^2 \right\rangle_q = \exp\left[2(\sigma/\tau_{in})^2 - 2(t-t_0)/\tau_{in}\right] \frac{1+\mathrm{erf}\left[\frac{-2\sigma^2+(t-t_0)\tau_{in}}{\sqrt{2}\sigma\tau_{in}}\right]}{\mathrm{erfc}\left(-\frac{t-t_0}{\sqrt{2}\sigma}\right)}. \tag{11}$$

In the case of many afferents, the total postsynaptic current is $I(t) = I_{peak} \sum_{i=1}^{\nu(t)} q_i(t)$. Here, $1 \leq \nu(t) \leq M$ is the fraction of the M afferents in

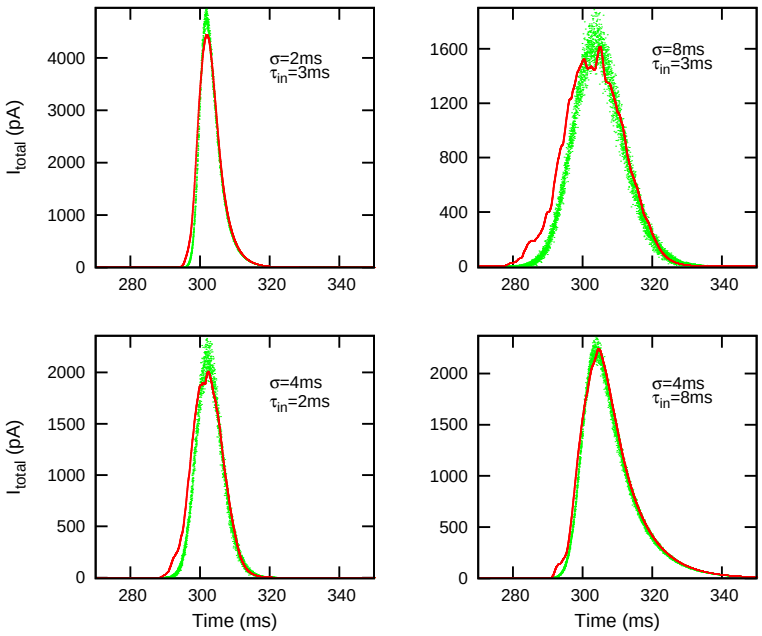

Figure 8: Excitatory postsynaptic current generated in a neuron which receives an single AP through $M = 200$ synapses. In each presynaptic neuron, the AP occurs at different times t_i which are Gaussian distributed around $t_0 = 300ms$. The figure shows that the effect of jitter is the spreading of the current curve, whereas an increment in the inactivation time constant causes longer right tails. Numerical results (lines) are in concordance with the analytical derivation of the current (dots) (see main text for an explanation).

which the AP has already generated a postsynaptic response at time t, and it is given by $\nu(t) \approx M \int_{-\infty}^{t} p(t_i)dt_i$. This number depends on time due to the existence of the jitter that desynchronizes the postsynaptic effect of the AP in all afferents. For $t \ll t_0$, $\nu(t)$ is, therefore, small but for t near to and large than t_0, $\nu(t)$ is high and we can use the central limit theorem to obtain:

$$I(t) = I_{peak}\xi(t, t_0), \tag{12}$$

where $\xi(t, t_0)$ is a Gaussian variable with mean and variance given by

$$\langle \xi(t, t_0) \rangle_\xi = \nu(t) \langle q(t) \rangle_q \tag{13}$$

and

$$\sigma_\xi^2 = \nu(t)[\langle q^2(t) \rangle_q - \langle q(t) \rangle_q^2], \tag{14}$$

with $\nu(t) = \frac{M}{2}\left[\text{erf}\left(\frac{t-t_0}{\sigma}\right) + 1\right]$. We will use, hereafter, this analytical approach to compute CD maps of a jittered signal.

Since $\nu(t)$ needs to be high to use the central limit theorem, one expects that the theoretical current defined by equations (12-14) will fit better the numerical results for $t > t_0$. In fact, this is depicted in Fig. 8, where the analytically

computed current after the arrival of M jittered APs (grey dots) is compared with the simulated current (red curve), for different values of the jitter σ and different values of the inactivation time constant τ_{in}. The figure shows the good agreement between the theoretically and numerically computed currents. One observes, moreover, that the effect of increasing the jitter is the temporal spreading of the current so that the signal influence occurs during a large period of time but with a smaller amplitude. This will cause a small decreasing in the capacity of the system to detect spikes. On the other hand, if we fix the jitter the effect of increasing τ_{in} is the appearance of longer tails for $t > t_0$, which would be a desirable effect since the response to the next incoming AP will be higher. However, no changes are detected in the amplitude of the current when τ_{in} is modified. Note that the effect of jitter does not depend on other parameters driving the dynamics of synapses, as U_{SE}, τ_{rec} or τ_{fac}, which only affect to the amplitude I_{peak} (see the appendix). One should not expect, therefore, a strong effect of jitter on the emergent properties due to facilitation and/or depression.

In order to compute CD maps, we have to calculate the voltage generated by the jittered signal, so that we have to integrate the Langevin equation

$$\tau_m \frac{dV}{dt} = -V + R_{in} I_{peak} \sum_{t_0} \xi(t, t_0). \tag{15}$$

Here the sum extends to a train of *events,* each one consisting of M jittered AP centered around a particular instant of time t_0 in the event train. In order to give a first approximation to the solution of this equation, the fluctuations are neglected. Therefore, the factor $\xi(t, t_0)$ is now a Gaussian function of time, centered at t_0 for each event in the train. Using standard methods and assuming a periodic train of events that occur at times $t_0 = 0, 1/f, 2/f, \ldots$, one can easily integrate the equation (15) to obtain

$$V(t) = \exp(-t/\tau_m) \left[\exp(-1/f\tau_m) \frac{W(1/f)}{1 - \exp(-1/f\tau_m)} + W(t) \right] \tag{16}$$

where

$$W(t) = \frac{R_{in}}{\tau_m} \int_0^t \exp(t'/\tau_m) I(t') dt' \tag{17}$$

and

$$I(t) = I_{peak} \langle \xi(t, 0) \rangle , \tag{18}$$

which determines the temporal evolution of the postsynaptic membrane potential. Simulations show that this expression is also valid for Poisson distributed event trains (data not shown). One can use (16) then to evaluate the CD maps similarly to the case of $\sigma = 0$ (non-jittered events). Indeed, as it is shown in the appendix, to do that is necessary the evaluation of the maximum value of $V(t)$ generated by the signal term, i.e. V_m, during the signal event duration. In the practice, this can be analytically done only in the case of $\sigma = 0$. For $\sigma \neq 0$, V_m must be numerically computed from (16).

The maps for the detection of strongly jittered events ($\sigma = 3\ ms$) are presented in Fig. 9 (top panels), for the case of only depressing (left) and depressing-facilitating synapses (right). An important conclusion is that the CD maps here are qualitatively the same than those obtained previously in the

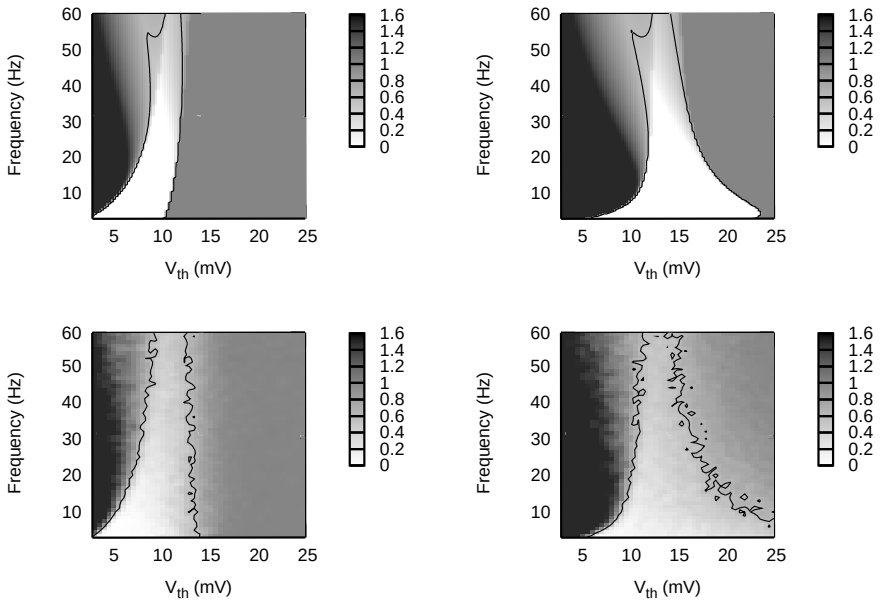

Figure 9: The effect of jitter and synaptic fluctuations on coincidence detection maps. Top panels shows CD maps corresponding to highly jittered signals ($\sigma = 3\ ms$) for only-depressing (left panel, $\tau_{fac} = 0$) and depressing-facilitating synapses (right panel, $\tau_{fac} = 1000\ ms$). The maps have been obtained with the postsynaptic membrane potential computed with the expression (16). The effect of the jitter is a small and non-relevant decreasing of the good CD regions. Other synapse parameters were $A_{SE} = 42\ pA$, $\tau_{rec} = 800\ ms$ and $U_{SE} = 0.1$. The bottom panels show the same CD maps obtained with a stochastic synapse model assuming six functional contacts per synapse and one released vesicle per functional contact. Similarly to top panels, differences between only-depressing (left, $\tau_{fac} = 0\ ms$) and depressing-facilitating synapses (right panel, $\tau_{fac} = 1300\ ms$) are shown. Other synapse parameters in this case were $A_{SE} = 32\ pA$, $\tau_{rec} = 200\ ms$ and $U_{SE} = 0.02$. In all panels, the solid line delimits regions where $E(f, V_{th}) < 0.6$ (light areas).

zero-jitter case (cf. Fig. 3). Increasing the value of the jitter yields to a decreasing of the area of good performance, as one could expect. This effect in the light zone is not too dramatic for $\sigma \lesssim 4$, however. The jitter also causes a small delay to reach the membrane threshold, as it is shown in Fig. 8 where one has the event at $t_0 = 300\ ms$ and the maximum of the generated current occurs at $t = t_0 + \delta t$. This fact turns into an increment in the number of failures and false hits. This effect should be considered in the numerical counting of hits, failures and falses, specially for high values of the jitter.

Other possible source of noise to consider in our signal-detection analysis is the existence of fluctuations during synaptic transmission due, mainly, to the

intrinsic dynamics of the synapses. For this, we used the model of stochastic transmission in individual synapses reported in (de la Rocha and Parga, 2005), which accounts the release of neurotransmitters in a single synapse as a stochastic event. The CD maps obtained using this model are shown in Fig. 9 (bottom panels), for only-depressing (left) and depressing-facilitating (right) synapses. For a comparison with top panels, in this model we chose parameters $A_{SE} = 32\ pA$, $U_{SE} = 0.02$ and $\tau_{rec} = 200\ ms$, which are within the physiological range (Markram et al., 1998). We make this choice to obtain the same qualitatively behaviour than the previous model with jittered signals, for the case of depressing synapses. Although this stochastic model introduces additional source of noise which makes the input-output correlation weaker and, therefore, the error in detection is slightly higher, one can see that the effect of including facilitation is also the same. That is, it induces the spreading of the region of good detection (light area) towards high threshold values.

We conclude, therefore, that results obtained in the previous section, are robust for a more realistic treatment of the input presynaptic trains, including the case of jittered signals, and more realistic model of synapses with realistic stochastic release of neurotransmitters.

5 Detection of presynaptic firing rate changes

In the previous studies, we have considered the overall presynaptic firing rate as a fixed parameter. This assumption is not realistic and, more interesting, is to consider the firing rate as a dynamic variable, as it happens in real neuronal tissue. The rate changes in the presynaptic neuron, during normal functioning, leads to a transient behaviour in the excitatory postsynaptic potential (EPSP) which could cause a burst or an AP in the postsynaptic neuron (Tsodyks and Markram, 1997; Pantic et al., 2003; Abbott et al., 1997). The question that arises then is if the postsynaptic neuron is able to detect synchronous changes (increases) in the afferent firing rates. This property have been found, in previous works, only for depressing synapses and not for static synapses (Pantic et al., 2003). Another question is if synaptic facilitation could have some positive effect in the detection of these rates changes by the postsynaptic neuron. In this section we try to answer these questions by studying the effect of increasing facilitation in spite of depression in the optimal detection of rate changes in the presynaptic neurons.

To start, we assume a population of $N = 1000$ afferents firing uncorrelated Poisson spike trains with a certain frequency f into a postsynaptic neuron. This population changes its mean firing rate every $1000\,ms$. Figure 10 shows a comparison in the output of the postsynaptic neuron for facilitating and depressing synapses. The threshold for firing was fixed in $V_{th} = 17\,ms$ and $U_{SE} = 0.1$. Simulations show that facilitating synapses ($\tau_{fac} = 500\,ms$) allow for a better detection of rate changes, and over a larger range of frequencies, than depressing synapses. In general, the regions in which depressing and facilitating synapses perform well can vary and this strongly depends on the given values of U_{se}, τ_{rec} and τ_{fac}. Thus, there are special situations where facilitation is needed to detect presynaptic rate changes and vice versa.

A simple theoretical approach, which has been used previously in the case of depressing synapses (Pantic et al., 2003) and agrees qualitatively with sim-

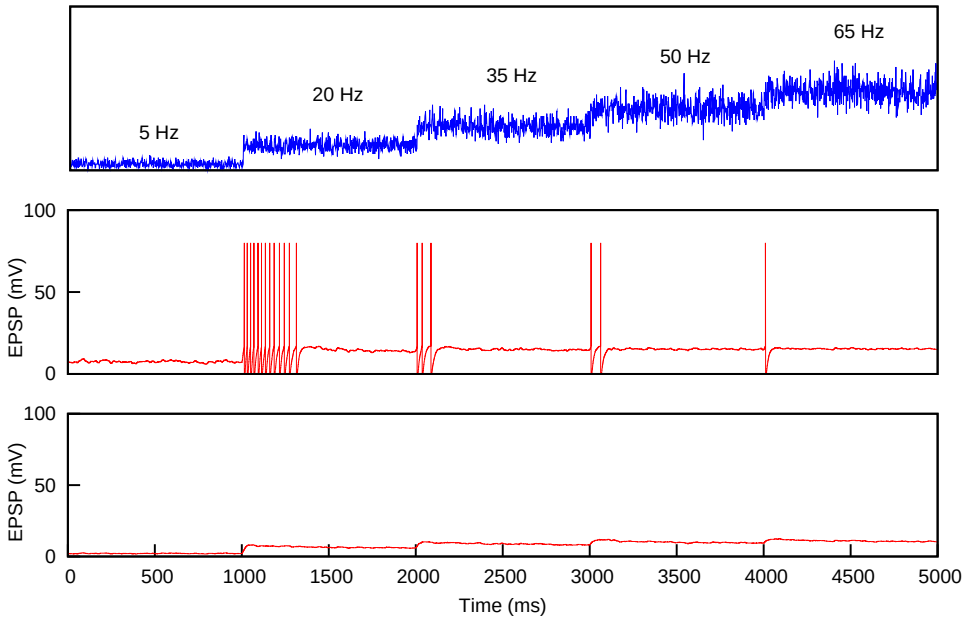

Figure 10: Detection of firing rate changes with depressing and facilitating synapses. The top panel shows the mean firing rate of the $N = 1000$ presynaptic neurons as a function of time. Middle and bottom panels show the response of the postsynaptic membrane potential for facilitating and depressing cases, respectively. In these simulations parameters were $U_{SE} = 0.1$ and $\tau_{fac} = 500\,ms(0\ ms)$ for the facilitating (depressing) case, respectively. Detection of variations onto lower frequencies are not possible with these synaptic mechanisms.

ulations (data not shown), can help us to find the regions in which firing rate changes are detected. To obtain such transient behaviour, which allows rate-change detection, the threshold of the postsynaptic neuron must satisfy $Cf_2\omega(f_1) > V_{th} > Cf_2\omega(f_2)$, where f_1 is the initial rate, f_2 is the firing rate after the change, $C = R_{in}N\tau_{in}$ and $\omega(f)$ is the stationary postsynaptic current strength for a given frequency. From the system of equations (1) and following a reasoning similar to the strategy used in the appendix, one can easily obtain

$$\omega(f) = \frac{A_{SE}U_\infty}{1 + f\tau_{rec}U_\infty} \tag{19}$$

where U_∞ is the steady state valued of $U(t)$ (see the appendix). If now we fix the frequency step $\delta f = f_2 - f_1$, the resulting expressions will only depend on f_1. Since for large enough frequencies $Cf_2\omega(f_1)$ is a decreasing function of f_1 and $Cf_2\omega(f_2)$ is an increasing function of f_2 (and therefore of f_1), these two tendencies will converge for some f_1. This leads to a close area of good rate change detection between the two curves. These two theoretical functions depends on the synapse relevant parameters and, therefore, allows for a theoretical

treatment of the regions in which firing rate changes can be detected, depending on the balance between depression and facilitation.

6 Discussion

Recently, there was an increasing interest in the study of the computational functionality of activity dependent synaptic processes as facilitation and depression in actual neural systems and neural networks models (Abbott and Regehr, 2004; Destexhe and Marder, 2004; Pantic et al., 2002; Pantic et al., 2003). It has been reported, for instance, that these processes can affect the stability of the dynamical attractors of neural network models, and as a consequence, an oscillatory phase emerges with the activity of the network visiting all attractors (Pantic et al., 2002; Cortes et al., 2006; Torres et al., 2007). This jumping behavior could explain, for instance, the appearance of voltage transitions between up and down states observed in cortical areas (Holcman and Tsodyks, 2006).

In this work, we have presented a detailed theoretical and numerical study of how the competition between synaptic facilitation and depression affects the neural detection of temporal correlations between different presynaptic neurons in a background of uncorrelated noise. Our study shows that the inclusion of the facilitation mechanisms enhances the performance of cortical neural systems to perform this task, for a wide range of frequencies and neuron thresholds and for any possible values of the parameters which define the dynamics of the synapses, namely, U_{SE}, τ_{fac} and τ_{rec}. In particular, we have shown that the transmission of information, codified in spike trains through the synapses, is enhanced and the detection of firing rate changes is also improved compared with the case of only depressing synapses. Thus, contrary to what happens with only depression, the presence of facilitation makes not necessary to have a high value for the maximum amount of active neurotransmitters to efficiently detect correlated signals. This would lead us to think that facilitation has a crucial role in the processing of information through synapses even when the neuron does not have enough synaptic resources.

Facilitation also determines the existence of an optimal frequency which allows good performance for a wide range of neuron firing thresholds. In particular, these results could be important to understand how actual neural systems –where different types of neurons with non-identical firing thresholds are connected in a complex way– can self-organize to efficiently detect and process relevant information (Azouz and Gray, 2000). Thus, the existence of this optimal frequency could be related with recent experimental findings which reveals the existence of similar optimal frequencies in the presence of facilitation in the heterogeneous pyramidal network of the prefrontal cortex (Wang et al., 2006).

We have also seen that, although important, it is not crucial to have a strong correlation between the different presynaptic afferents to have a good detection of signals, and our results also fulfill for noisy signals. This is of special relevance since it is well known that the intrinsic stochasticity of actual synapses causes fluctuations that disrupt the synchrony between the afferents and produce a highly fluctuating postsynaptic response (Dobrunz and Stevens, 1997). To account for that more precisely, we have study the role of the balance between synaptic facilitation and depression with a more realistic stochastic model of synaptic transmission (de la Rocha and Parga, 2005). The results of

this analysis have shown that our main conclusions also fulfill for this case.

7 Acknowledgments

This work was supported by the *MEyC–FEDER* project FIS2005-00791 and the *Junta de Andalucía* project FQM–165. We thank useful discussion with J. Marro.

Appendix

Analytical derivation of the error function $E(f, V_{th})$

In this section we derived analytical expressions for the functions appearing in the definition of the error function (5) used to obtain theoretically the regions for good spike coincidence detection in the $(f, V_{\rm th})$ parameter space.

First, we assume that the total presynaptic current can be divided in two terms: a signal term containing the correlated embedded signal and a noise term formed by the background of uncorrelated spikes.

Noise contribution

To take into account the noise generated by $N - M$ uncorrelated spikes trains, we assume that the current at time $t = t^* + \tau$ generated by a single spike arriving to the synapse i at time t^* is given by

$$I_i(\tau, t^*) = I_{peak} \exp(-\tau/\tau_{in}) \tag{20}$$

where I_{peak} represents the averaged stationary EPSC amplitude obtained after stimulation with a periodic spike train, assumption that we also suppose valid for Poisson distributed spike train. After this consideration, one easily obtains from equations (1-3) that

$$I_{peak} = A_{SE} \frac{U_\infty (1 - \exp(-1/f\tau_{rec}))}{1 - (1 - U_\infty) \exp(-1/f\tau_{rec})} \tag{21}$$

with $U_\infty = u_\infty(1 - U_{SE}) + U_{SE}$, where u_∞ is the value of $u(t)$ in the stationary state ($t \to \infty$). For a periodic spike train, u_∞ is given by

$$u_\infty = U_{SE} \frac{\exp(-1/f\tau_{fac})}{1 - (1 - U_{SE}) \exp(-1/f\tau_{fac})}. \tag{22}$$

We can compute the mean noise contribution of the current and fluctuations using the standard expressions

$$\begin{array}{ll} I_{noise} & \equiv \langle I \rangle, \\ \sigma^2_{I_{noise}} & \equiv \langle I^2 \rangle - \langle I \rangle^2 \end{array} \tag{23}$$

From these definitions and using the central limit theorem we obtain

$$I_{noise} = (N - M) A_{SE} f \tau_{in} U_\infty \frac{1 - \exp(-1/f\tau_{rec})}{1 - (1 - U_\infty) \exp(-1/f\tau_{rec})} \tag{24}$$

where we assumed that $\tau_{in} \ll \tau_{rec}$.

If we neglect fluctuations ($\sigma_{I_{noise}} = 0$), we can write $V_{noise} = R_{in} I_{noise}$. Using this expression one can compute N_{falses} taken into account that false firing occurs when $V_{noise} > V_{th}$ so by a direct integration of equation (4) in a period of time T gives $N_{falses} \approx T/\{\tau_{ref} - \tau_m \ln(1 - V_{th}/V_{noise})\}$ (Koch, 1999). Now using that $f = N_{inputs}/T$, we finally obtain as in (Pantic et al., 2003)

$$N_{falses} = \frac{\theta(V_{noise} - V_{th}) N_{inputs}}{f(\tau_{ref} - \tau_m \ln(1 - V_{th}/V_{noise}))} \tag{25}$$

where $\theta(x)$ is the Heaviside step function, which takes into account that for $V_{noise} < V_{th}$ $N_{falses} = 0$.

To take into account fluctuations of I_{noise} one can use the so called hazard function approximation (Plesser and Gerstner, 2000) but it has been reported that it gives the same results than those obtained using the formula (25) for high frequencies and, on the contrary to the expression (25), it does not work properly for small frequencies (Pantic et al., 2003). Therefore, hereafter we will neglect fluctuations in I_{noise} and use (25) as an approximatively valid expression to analytically compute N_{falses}.

Signal contribution

To analyse the signal contribution (arising from M coincident spikes) we used the same method developed in (Pantic et al., 2003) for the case of only depressing synapses. That is, assuming that $V(0; t^*)$ is the membrane potential at $t = t^*$ when M coincident spikes arrive, by direct integration of the equation (4) the membrane potential at time $t = t^* + \tau$ is

$$V(\tau; t^*) = e^{\tau/\tau_m} \left\{ V(0; t^*) + \frac{R_{in} M I_{peak}}{\tau_m \alpha} [e^{\alpha\tau} - 1] \right\} \tag{26}$$

where $\alpha = \frac{\tau_{in} - \tau_m}{\tau_{in}\tau_m}$ and I_{peak} is given by (21) including all the effects due to synaptic depression and facilitation. If the next signal event (M coincident spikes) occurs at $t = t'$ one can obtain the following recurrence relation:

$$V(0; t') = e^{\Delta t/\tau_m} \left\{ V(0; t^*) + \frac{R_{in} M I_{peak}}{\tau_m \alpha} [e^{\alpha \Delta t} - 1] \right\} \tag{27}$$

with $\Delta t = t' - t^*$. which allows for computing the stationary value for the membrane potential at the exact time of the signal event arrival (see also (Kistler and van Hemmen, 1999)), that is:

$$V_{st} = e^{-\Delta t/\tau_m} \frac{R_{in} M I_{peak}}{\tau_m \alpha} \frac{e^{\alpha \Delta t} - 1}{(1 - e^{-\Delta t/\tau_m})}. \tag{28}$$

We define V_{signal} as the maximum of the membrane potential reached between the arrival of two consecutive signal events separated by a time Δt. This can be easily computed from equation (26) with $V(0, t^*)$ replaced V_{st}:

$$V_{signal} = \left[\frac{\tau_m (1 - \exp(-1/f\tau_m))}{\tau_{in} (1 - \exp(-1/f\tau_{in}))} \right]^{\frac{\tau_m}{\tau_{in} - \tau_m}} R_{in} M I_{peak} \tag{29}$$

where we consider $\tau = \Delta t \backsimeq 1/f$.

The expression of V_{signal} allows for an evaluation of the number of failures assuming that $N_{failures} = N_{inputs} - N_{hits}$. Then, one obtains by direct integration of equation (4) an using the same reasoning that for N_{false} case that

$$N_{failures} = N_{inputs}\left[1 - \frac{\theta(V_{noise} + V_{signal} - V_{th})}{f[\tau_{ref} - \tau_m \ln(1 - (V_{th} - V_{signal})/V_{noise})]}\right] \quad (30)$$

where we have considered a hit event every time $V_{noise} + V_{signal}$ reach V_{th}. Note that from (30) if $V_{noise} + V_{signal} < V_{th}$ we will have $N_{failures} = N_{inputs}$.

Expression for N_{falses}, $N_{failures}$ allows for theoretically compute the number of errors in the CD maps.

References

Abbott, L. F. and Regehr, W. G. (2004). Synaptic computation. *Nature*, 431:796–803.

Abbott, L. F., Varela, J. A., Sen, K., and Nelson, S. B. (1997). Synaptic depression and cortical gain control. *Science*, 275(5297):220–224.

Azouz, R. and Gray, C. M. (2000). Dynamic spike threshold reveals a mechanism for synaptic coincidence detection in cortical neurons in vivo. *Proc. Natl. Acad. Sci. USA*, 97(14):8110–8115.

Bertram, R., Sherman, A., and Stanley, E. F. (1996). Single-domain/bound calcium hypothesis of transmitter release and facilitation. *J. Neurophysiol.*, 75:1919–1931.

Buia, C. I. and Tiesinga, P. H. E. (2005). Rapid temporal modulation of synchrony in cortical interneuron networks with synaptic plasticity. *Neurocomputing*, 65-66:809–815.

Cortes, J. M., Torres, J. J., Marro, J., Garrido, P. L., and Kappen, H. J. (2006). Effects of fast presynaptic noise in attractor neural networks. *Neural Comp.*, 18:614–633.

de la Rocha, J. and Parga, N. (2005). Short-term synaptic depression causes a non-monotonic response to correlated stimuli. *J. Neurosci.*, 25:8416–8431.

Destexhe, A. and Marder, E. (2004). Plasticity in single neuron and circuit computations. *Nature*, 431:789–795.

Dobrunz, L. E. and Stevens, C. F. (1997). Heterogeneity of release probability, facilitation, and depletion at central synapses. *Neuron*, 18:995–1008.

Holcman, D. and Tsodyks, M. (2006). The emergence of up and down states in cortical networks. *PLoS Comput. Biol. 2(3)*, 2(3):174–181.

Hopfield, J. J. (1982). Neural networks and physical systems with emergent collective computational abilities. *Proc. Natl. Acad. Sci. USA*, 79:2554–2558.

Kistler, W. and van Hemmen, J. (1999). Short-term synaptic plasticity and network behavior. *Neural Comp.*, 11:1579–1594.

Koch, C. (1999). *Biophysics of Computation: Information Processing in Single Neurons*. Oxford University Press.

Markram, H., Wang, Y., and Tsodyks, M. (1998). Differential signaling via the same axon of neocortical pyramidal neurons. *Proc. Natl. Acad. Sci. USA*, 95:5323–5328.

Matveev, V. and Wang, X. J. (2000). Differential short-term synaptic plasticity and transmission of complex spike trains: to depress or to facilitate? *Cerebral Cortex*, 10:1143–1153.

McAdams, C. and Maunsell, J. (1999). Effects of attention on orientation-tuning functions of single neurons in macaque cortical area v4. *Journal of Neuroscience*, 19:431–441.

Pantic, L., Torres, J. J., and Kappen, H. J. (2003). Coincidence detection with dynamic synapses. *Network: Comput. Neural Syst.*, 14:17–33.

Pantic, L., Torres, J. J., Kappen, H. J., and Gielen, S. C. A. M. (2002). Associative memmory with dynamic synapses. *Neural Comp.*, 14:2903–2923.

Plesser, H. E. and Gerstner, W. (2000). Noise in integrate-and-fire neurons: from stochastic input to escape rates. *Neural Comp.*, 12:367–384.

Torres, J. J., Cortes, J., Marro, J., and Kappen, H. (2007). Competition between synaptic depression and facilitation in attractor neural networks. *Neural Comp.* In press, q-bio.NC/0604019.

Tsodyks, M. V. and Markram, H. (1997). The neural code between neocortical pyramidal neurons depends on neurotransmitter release probability. *Proc. Natl. Acad. Sci. USA*, 94:719–723.

Tsodyks, M. V., Pawelzik, K., and Markram, H. (1998). Neural networks with dynamic synapses. *Neural Comp.*, 10:821–835.

Wang, Y., Markram, H., Goodman, P. H., Berger, T. K., Ma, J., and Goldman-Rakic, P. S. (2006). Heterogeneity in the pyramidal network of the medial prefrontal cortex. *Nature Neurosci.*, 9:534–542.